JOURNAL OF AGRICULTURAL AND FOOD CHEMISTRY
ARTICLE

J. Agric. Food Chem. 2009, 57, 10565–10572 10565
DOI:10.1021/jf902597w

Enhancement of Antitumor Activities in Sulfated and Carboxymethylated Polysaccharides of *Ganoderma lucidum*

Jianguo Wang,[†] Lina Zhang,*[,†] Yonghui Yu,[‡] and Peter C. K. Cheung[§]

[†]Department of Chemistry, Wuhan University, Wuhan 430072, People's Republic of China, [‡]Open Laboratory for Oversea Scientists, Center for Medical Research, Wuhan University, Wuhan 430071, People's Republic of China, and [§]Department of Biology, The Chinese University of Hong Kong, Hong Kong, People's Republic of China

Two water-soluble derivatives, sulfated and carboxymethylated *Ganoderma lucidem* polysaccharides, coded as S-GL and CM-GL, were prepared using derivatization of water-insoluble polysaccharides (GL-IV-I) extracted from the fruit body of *G. lucidem*. The degree of substitution (DS) of S-GL and CM-GL was 0.94 and 1.09, respectively. The weight-average molecular mass (M_w) of GL-IV-I, S-GL, and CM-GL was determined with light scattering to be 13.3×10^4, 10.1×10^4, and 6.3×10^4, respectively. S-GL and CM-GL inhibited the *in vitro* proliferation of Sarcoma 180 (S-180) tumor cells in a dose-dependent manner, with an IC_{50} value of 26 and 38 μg/mL, respectively. They also inhibited the growth of S-180 solid tumors implanted in BALB/c mice, with low toxicity to the animals. Flow cytometric studies revealed that treatment of S-GL and CM-GL with S-180 tumor cells could mediate the cell-cycle arrest in the G_2/M phase. The expression of Bax increased, and the expression of Bcl-2 decreased dramatically, as shown by immuno-histochemical staining of S-180 tumor tissue excised from the animals. The sulfated and carboxmethylated groups in the polysaccharides played an important part in enhancing their antitumor activities, leading to the potential to be developed into antitumor drugs.

KEYWORDS: Polysaccharide conformation; antitumor activities; sulfated derivative; carboxymethylated derivative; cell-cycle; apoptosis

INTRODUCTION

The global awareness of cancer as one of the leading causes of death in people of various ages and racial backgrounds has led to a great deal of research efforts and clinical studies in the fight against the disease (*1*). Therefore, searching for anticancer drugs with higher bioactivities and lower toxicity from nature has been an extremely active domain. Nowadays, development of noninvasive treatments of cancer is required because the traditional cancer treatments are often toxic to normal cells and can cause serious side effects (*2*). Natural products from plants, microorganisms, and marines are safe, biocompatible, and biodegradable and have bioactivities, such as antioxidantion and immunostimulatory effects (*3*−*5*). Mushroom, non-starch polysaccharides, have been considered as natural antitumor agents, having tumor-specific and immunomodulatory effects. It has been suggested that the action of antitumor activities of polysaccharides are not only immunomodulatory but may also result from a direct cytotoxic effect on the tumor cells. It is generally believed that polysaccharides do not induce direct toxicity on tumor cells, and little is known about its exact mechanism (*6*, *7*). To effectively research and develop natural anticancer drugs, it is necessary to elucidate the mechanism of the antitumor activities of polysaccharides with an understanding of the effect of their chemical structure, molecular weight, and chain conformation.

Ganoderma lucidum polysaccharides, one of the main efficacious ingredients of *G. lucidum* (Leyss, ExFr.) Karst (Gl), has been under modern pharmacological research in recent 30 years and has been reported to be effective in inhibiting tumor growth (*8*). Its fruit body has long been used as a traditional Chinese medicine to promote health and longevity, coded as "elixir of youth" by ancient emperors. The earliest record of "Lingzhi" was in the "Shen Nong's Materia Medica" in the Han Dynasty of China about 2000 years ago. However, the polysaccharides extracted with alkali from *G. lucidum* are mainly water-insoluble (1 → 3)-β-D-glucan and less suitable for pharmaceutical study because of its poor water solubility. In the last few decades, much attention has focused on the biological properties of polysaccharides and their chemical derivatives, especially sulfated and carboxymethylated derivatives (*9*). It has been demonstrated that chemical sulfation and carboxymethylation of water-insoluble polysaccharide should not only enhance the water solubility but also change the chain conformation, resulting in the improvement of their biological activities (*10*−*12*). The objective of this work was to prepare sulfated and carboxymethylated derivatives from water-insoluble polysaccharides extracted from the fruit body of *G. lucidum*. Moreover, we investigated the effects of these two derivatives on inhibiting cellular proliferation, cell-cycle progression, and apoptosis against Sarcoma 180 (S-180) tumor

*To whom correspondence should be addressed. Telephone: +86-27-87219274. Fax: +86-27-68754067. E-mail: lnzhang@public.wh.hb.cn.

Published on Web 10/28/2009

to evaluate their bioactivities. This work can provide important insight for the introduction of the charged group to polysaccharides upon the enhancing of their antitumor activities and induction of apoptosis.

MATERIALS AND METHODS

Preparation of Derivatives and Characterization. A linear water-insoluble (1 → 3)-β-D-glucan, coded as GL-IV-I, was isolated from the fruit body of *G. lucidum* by extracting with sodium hydroxide solution (*13*). The GL-IV-I polysaccharide was sulfated and carboxymethylated separately, coded as S-GL and CM-GL, respectively, according to the procedures of Yoshida et al. and Bao et al. (*14*, *15*). Both of these two derivatives were white scale-like samples. The degree of substitution (DS) in the above two derivatives was determined with element analysis by the following equation:

$$DS = (162 \times W\% - M_a)/(W_a - M_s \times W\%) \quad (1)$$

where M_a is the total atomic weight of the element from the original sugar unit, W_a is the total atomic weight of the element from the substitution group, and M_s is the molecular mass of a substitution group.

Infrared (IR) spectra of the samples were carried out with a Nicolet Fourier transform infrared (FTIR) spectrometer (Spectrum One, Thermo Nicolet Co., Madison, WI) in the range of 4000−400 cm^{-1} using the KBr disk method. High-resolution ^{13}C nuclear magnetic resonance (NMR) was carried out with a Mercury 500 NMR spectrometer (Varian, Inc., Palo Alto, CA) at room temperature. The concentrations of the GL-IV-I and its derivatives were adjusted to 100 mg/mL for NMR experiments. Me_2SO-d_6 was used as a solvent for GL-IV-I, and 99.96% D_2O was used as a solvent for the derivatives.

Size-exclusion chromatography combined with multi-angle laser light scattering (SEC−LLS, λ = 633 nm Optilab, DAWN DSP, Wyatt Technology Co., Santa Barbara, CA) measurements of the samples were carried out to obtain the molecular mass of the samples. A P100 pump (Thermo Separation Products, San Jose, CA) equipped with columns of G4000PWXL (MicroPak, TSK) in 0.9% NaCl aqueous solution and a column of G4000HXL in Me_2SO at 25 °C was used as the SEC instrument. A differential refractive index detector (RI-150, Thermo Separation Products, San Jose, CA) was simultaneously connected. The carrier solutions were 0.9% NaCl aqueous solution and Me_2SO. The solvents and polysaccharide solutions were purified by a 0.2 μm filter and degassed before use. The injection volume was 200 μL, with a concentration of 3 mg/mL for the sample, and the flow rate was 0.5 mL/min in 0.9% NaCl aqueous solution and 0.5 mL/min in Me_2SO. Astra software (version 4.90.07) was used for data acquisition and analysis.

Cytotoxicity and Cell Viability Analysis. Sarcoma tumor cell line (kindly provided by Tongji Medical College of the Huazhong University of Science and Technology) was used to test the *in vitro* and *in vivo* antitumor activities of the sample. Cells were grown in Roswell Park Memorial Institute (RPMI) 1640 medium supplemented with 10% fetal bovine serum (FBS), 100 μg/mL streptomycin, and 100 units/mL penicillin. Cell viability of control and treated cells was evaluated using the 3-(4,5-dimethylthiazol-2-yl)-2,5-diphenyltetrazolium bromide (MTT) assay in triplicate. Briefly, an amount of 1×10^4 cells was seeded in each well of a 96-well microplate. The cells were permitted to adhere for 24 h and washed with phosphate buffer solution (PBS), and fresh medium was added and then treated with S-GL and CM-GL, dissolved in medium at the final concentration range of 1−500 μg/mL (*16*). The treated cells were incubated for 24 h at 37 °C in a humidified atmosphere of 5% carbon dioxide. After treatment, the culture medium was replaced by fresh medium. Then, cells in each well were incubated at 37 °C in 50 μL of MTT (5 mg/mL) for 4 h. After the medium and MTT were removed, 200 μL of Me_2SO and 25 μL of glycine buffer (0.1 M glycine and 0.1 M NaCl at pH 10.5) were added to each well. Absorbance at 570 nm of the mixture was detected using a microplate ELISA reader (MRX II, DYNEX Technologies, Chantilly, VA). The absorbance of untreated cells was considered as 100%. The results were determined by three independent experiments. The relative cell viability was calculated as

$$\text{cell viability } (\%) = (OD_{570(\text{samples})})/(OD_{570(\text{control})}) \times 100 \quad (2)$$

where $OD_{570(control)}$ was obtained in the absence of polymers and $OD_{570(samples)}$ was obtained in the presence of polymers.

***In Vivo* Antitumor Activity Assay.** A total 32 BALB/c female mice, weighing 20.0 ± 2.0 g, were randomly divided into 4 groups (n = 8) and allowed free access to a standard laboratory diet and water. S-180 cells (about 1.5×10^6) were subcutaneously implanted into the right-hand groin of the mice. 5-Fluorouracil (5-Fu) and the tested polysaccharides were dissolved in 0.9% aqueous sodium chloride solution and were injected intraperitoneally daily (once starting 24 h after tumor inoculation). The same volume of 0.9% aqueous sodium chloride solution was injected intraperitoneally similar to the controlled group. After 8 days of administration, the tumors were removed from the mice and weighed. The tumor weight was compared to those in the controlled group of mice. The inhibition ratio (ξ) and the enhancement ratio of the body weight (φ) were calculated as follows:

$$\xi = [(W_c - W_t)/W_c] \times 100\% \quad (3)$$

$$\varphi = [(W_a - W_b)/W_b] \times 100\% \quad (4)$$

where W_c is the average tumor weight of the control group, W_t is the average tumor weight of the tested group, and W_a and W_b are the body weight of the mice after and before the treatment, respectively.

Cell-Cycle Analysis. The effects of S-GL and CM-GL on S-180 cell-cycle were assessed by flow cytometry. The cells (5×10^4 cells/mL) were incubated on a 6-well plate with polysaccharide samples (at final concentrations of 0.02 mg/mL) for 24 h. After the incubation, the cells were washed with phosphate-buffered saline (PBS) twice, fixed in 70% cold ethanol, and stored at −20 °C overnight. Prior the analysis, the fixed cells were washed with PBS twice and stained with 50 μg/mL propidium iodide (PI). The stained cells were then transferred to flow tubes by passing through nylon mesh with a pore size of 40 μm. Flow cytometric analysis was performed on a flow cytometer (Beckman Coulter, Epics XL MCL). Apoptotic cells were determined by their hypochromic sub-diploid staining profiles. The distribution of cells in the different cell-cycle phases was analyzed from the DNA histogram using Multicycle software (Phoenix Flow Systems, San Diego, CA)

Detection of Apoptosis. Shrinkage of cells and disorganization of chromatin are usually related to apoptosis. Simultaneous staining with Annexin V-FLOUS and PI distinguished between intact cells, early apoptosis, late apoptosis, or cell death (*6*). Annexin V-FLOUS, a calcium-dependent phospholipid binding protein with a high affinity for phosphatidylserine, was used to detect cell apoptosis. Treated S-180 cells (1.5×10^5) were plated onto a gelatinized culture flask in RPMI 1640 containing 20% fetal bovine serum (FBC) and incubated at 37 °C and 5% CO_2 for 24 h. The medium was replaced with 1 mL of RPMI 1640 with 5% FBC and polysaccharide samples (at final concentrations of 0.02 mg/mL) for 24 h and incubated at 37 °C and 5% CO_2 for 48 h. Treated and control S-180 cells were labeled with Annexin V-FLOUS (10 μg/mL) and PI (20 μg/mL) prior to harvesting. After labeling, all plates were washed with binding buffer and harvested by scraping. Cells were resuspended in binding buffer at a concentration of 2×10^5 cells/mL before analysis by flow cytometry (FACScan). Data analysis was performed using standard Cell Quest software (Becton-Dickinson).

Immunohistochemistry for Apoptosis-Related Proteins Bax and Bcl-2. The tests of Bax and Bcl-2 immunohistochemistry were performed by the peroxidase-labeled streptavidin−biotin method with microwave antigen retrieval (*17*−*19*). Paraffin in the sections were removed by treating with xylene for 15 min twice and then gradually hydrated through a series from 95, 80, to 70% of graded ethanol (2 min each) and distilled water (2 min). Endogenous peroxidase was blocked by incubation in 3% hydrogen peroxide (H_2O_2) for 10 min at 37 °C, followed by washing for 4 times with PBS (5 min each). Antigen retrieval was carried out in a microwave oven. Briefly, the sections were heated to 95 °C in 0.01 M citrate buffer (pH 6.0) and were maintained at this temperature for 10 min, followed by rinsing in warm tap water. Then, the sections were treated with normal goat serum for 10 min at 37 °C to reduce non-specific staining. Subsequently, the rabbit anti-mouse Bax and Bcl-2 polyclonal antibodies (Santa Cruz Biotechnology, Inc., Santa Cruz, CA) as primary antibodies were added in optimal dilution, and the sections were incubated overnight in a humidified chamber at 4 °C. This step and each of the following were

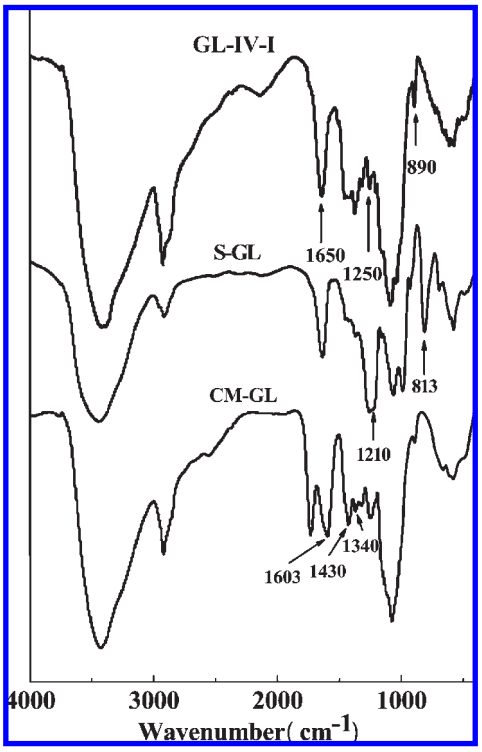

Figure 1. FTIR spectra of the native GL-IV-I and its sulfated (S-GL) and carboxymethylated (CM-GL) derivatives.

succeeded by washing for 4 times in PBS for 5 min each. The sections were incubated for 10 min at 37 °C in a humidified chamber with biotinylated goat anti-rabbit IgG (Zhongshan Golden Bridge Biotechnology Co., Ltd., Beijing, China; 1:200) as secondary antibodies, followed by exposure to streptavidin horseradish peroxidase (Zhongshan Golden Bridge Biotechnology Co., Ltd., Beijing, China) for 10 min at 37 °C. The color was developed using a solution containing 0.05% diaminobenzidine (DAB) as chromogen and 0.02% H_2O_2. After visualization of horseradish-peroxidase activity by color reaction with DAB, the sections were weakly counterstained with hematoxylin, mounted, and examined using a light microscope equipped with a 40× objective. To confirm immunospecificity, negative controls consisted of sections in which the primary antibody was omitted and replaced by a buffer or non-immune IgG. Formalin-fixed, paraffin-embedded sections of normal human lymph node served as positive controls. Both the number of immuno-reactive cells and the total number of cells (at least 500 cells) were determined to calculate the percentage of Bax and Bcl-2 positive cells by visual inspection of six different fields per section. To assess the apoptosis, ratios of Bcl-2/Bax were determined.

Statistical Analysis. The mean values and standard deviations of the data between the control and the treatment groups were analyzed by Dunnett's test, and the p values for any significant differences between means were set at less than 0.05. The flow cytometric analyses were repeated twice to confirm the findings.

RESULTS AND DISCUSSION

Chemical Structure. The FTIR spectra of the native GL-IV-I and its derivatives are shown in **Figure 1**. All samples exhibited the characteristic IR absorption of polysaccharides at 1250 and 1650 cm^{-1}.The native GL-IV-I exhibited absorption peaks at 890 cm^{-1}, which is the characteristic absorption peak of the β configuration of glucan (*20*). In comparison to GL-IV-I, the characteristic peak of the β configuration of S-GL at 890 cm^{-1} disappeared and two new absorption peaks at 813 and 1210 cm^{-1} appeared for the sulfated derivative, which corresponds to C−S−C symmetrical vibration and S=O asymmetrical stretching (*21*). This indicated that the sulfated derivative had been

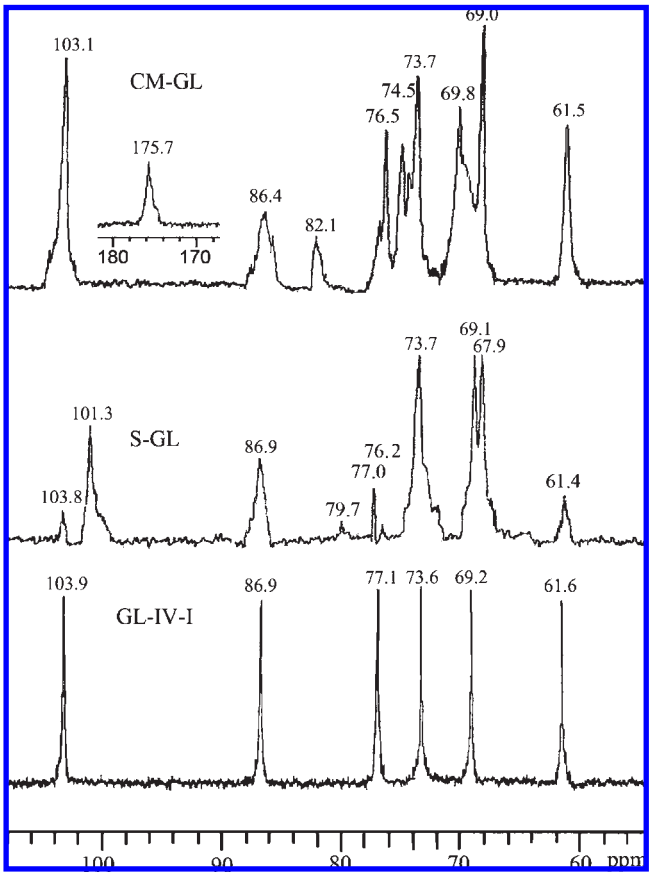

Figure 2. ^{13}C NMR spectra for native sample GL-IV-I in Me_2SO-d_6 and its sulfated (S-GL) and carboxymethylated (CM-GL) derivatives in D_2O at 25 °C.

Table 1. ^{13}C NMR Chemical Shifts for Native Sample GL-IV-I and Its Derivatives

	δ (ppm)											
sample	C-1	C-1′	C-2	C-2s	C-3	C-3′	C-4	C-4s	C-5	C-5′	C-6	C-6s
GL-IV-I	103.9		73.6		86.9		69.2		77.1		61.6	
S-GL	103.8	101.3	73.7	79.7	86.9		69.1	76.2	77.0	72.8	61.4	67.9
CM-GL	103.1		73.7	82.1	86.4	85.2	69.0	74.5	76.5	74.1	61.5	68.9

successfully synthesized from GL-IV-I. For CM-GL, two new absorption peaks appeared at 1603 and 1430 cm^{-1}, assigned to the asymmetrical −COO stretching vibration. The symmetrical −COO stretching and the new peak at 1340 cm^{-1} were assigned to the $-CH_2$ group (*22*−*25*).

The heteronuclear multiple-quantum coherence (HMQC) and double quantum filter (DQF) were described previously (*13*). The results could confirm that GL-IV-I was a linear (1 → 3)-β-D-glucan (*26*). The ^{13}C NMR spectra for the native sample GL-IV-I and its derivatives (S-GL and CM-GL) are shown in **Figure 2**, and their chemical shifts are listed in **Table 1**. The ^{13}C NMR spectrum of the native GL-IV-I exhibited six signals around 103.9, 86.9, 77.1, 73.6, 69.2, and 61.6 ppm, attributed to C-1, C-3, C-5, C-2, C-4, and C-6, respectively, indicating the characteristic of (1→3)-β-D-glucan (*22*). In comparison to the native GL-IV-I sample, there were several new signals caused by sulfated groups in S-GL. The peak at 67.9 was assigned to the signal of C-6s; the peak at 79.7 was assigned to the signal of C-2s; and the peak at 76.2 was assigned to the signal of C-4s. The peak at 61.4 was weakened, indicating that C-6 had been substituted by the sulfated group, whereas C-2 and C-4 have been partially substituted. Because

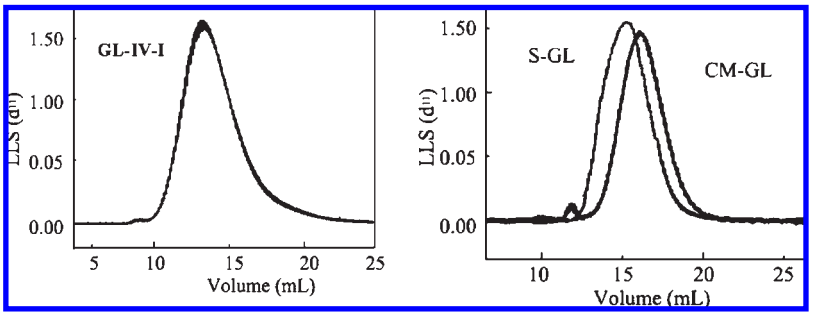

Figure 3. SEC patterns of GL-IV-I in Me_2SO (left) and its sulfated (S-GL) and carboxymethylated (CM-GL) derivatives in 0.9% NaCl aqueous solution (right) from LLS (detector 11) at 25 °C.

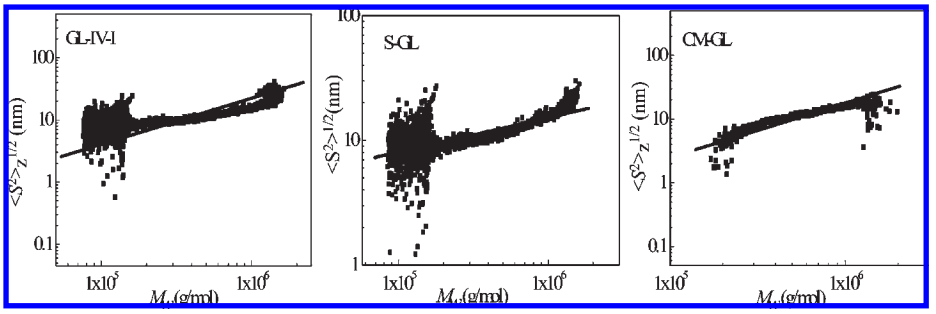

Figure 4. Dependence of $\langle S^2\rangle_z^{1/2}$ on M_w for GL-IV-I in Me_2SO and its sulfated (S-GL) and carboxymethylated (CM-GL) derivatives in 0.9% NaCl aqueous solution at 25 °C.

Table 2. Yield, Solubility, and DS for the Derivatives

		solubility[a]			DS from ^{13}C NMR			
sample	yield (%)	0.9% NaCl	Me_2SO	DS from EA result	C-6	C-4	C-2	total DS
GL-IV-I	7.6	−	+					
S-GL	86.3	++	−	0.94	0.68	0.12	0.08	0.88
CM-GL	95.1	++	−	1.18	0.62	0.28	0.19	1.09

[a] −, insoluble; +, soluble; ++, good solubility.

their strong peaks existed in the NMR spectrum, the peaks at 79.7 for C-2s and 76.2 for C-4s were much weaker than that of C-6s at 67.9. We could conclude that the C-6 position was more active than the C-2 and C-4 positions as a result of the steric hindrance (*27*). The downfield shift of the carbon atoms linked with the sulfur groups was about 6−7 ppm (*28*). Furthermore, a new peak appeared at 101.3, and the native C-1 peak at 103.8 became weaker in NMR spectra of S-GL. This could be explained by the fact that C-2 and C-6 had been substituted, which could influence the adjacent C-1 to split into two peaks. The upfield shift from C-1 to C-1′ was about 2.5 ppm, which is somewhat in line with the description by Gorin (*28*). With the same situation to C-5, the peak at 72.8 is for C-5′ of S-GL. In comparison to the native GL-IV-I, a new strong peak at 175.7 for CM-GL could be attributed to the C═O carbon of the carboxymethyl group, indicating the successful carboxymethylation of GL-IV-I. Peaks for C-6s, C-4s, and C-2s were at 69.0, 74.5, and 82.1, and the peak intensity was in the order C-6s > C-4s > C-2s. From ^{13}C NMR results, we could conclude that non-selectivity substitution occurred on the active hydroxyl groups of GL-IV-I and the multi-substitution at C-2, C-4, and C-6 exhibited different reaction activity. The yields, water solubility, and DS of the native polysaccharide and its derivatives are summarized in **Table 2**. The DS of the derivatives was calculated from the NMR data according to the method reported by Zhou et al. (*27*). In brief, the total DS of each kind of derivative was the summation of the DS for C-6, C-4, and C-2, and the relative DS values at the C-2, C-4, and C-6 positions were calculated from the relative intensities of peaks C-2, C-2s, C-4, C-4s, C-6, and C-6s. The DS of C-6, C-4, and C-2 calculated from ^{13}C NMR for S-GL and CM-GL were 0.68:0.12:0.04 and 0.62:0.28:0.19, respectively. Reaction activity of the active hydroxyl groups was in the order of C-6 > C-4 > C-2 on the whole. This could be explained by the fact that the steric hindrance led to the different activities of C-6, C-4, and C-2. The substitution further caused the adjacent C-1, C-3, and C-5 to split into two peaks, with the upfield shift of 2−3 ppm.

Molecular Mass and Chain Conformation. SEC−LLS, as an absolute method, is a convenient method for the determination of the true molecular mass and its distribution. The molecular mass and chain conformation parameters of GL-IV-I and its derivatives are summarized in **Table 3**. The SEC patterns of GL-IV-I in Me_2SO and the two derivatives in 0.9% NaCl aqueous solution analyzed by the LLS (detector d_{11} = 90°) at 25 °C are shown in **Figure 3**. Obviously, there were single peaks with good symmetry detected by LLS in GL-IV-I and its derivatives. The weight-average molecular mass (M_w) of GL-IV-I, S-GL, and CM-GL were 13.3 × 10^4, 10.1 × 10^4, and 6.3 × 10^4, respectively. The molecular mass of S-GL and CM-GL is lower than that of GL-IV-I because of the chain degradation during the reaction.

From the SEC chromatogram detected by LLS, we could obtain the M_w and $\langle S^2\rangle_z^{1/2}$ values of numberless fractions. The M_w−$\langle S^2\rangle_z^{1/2}$ relationship from many experimental points in the SEC can give conformation parameters (*29*). From data of M_w and $\langle S^2\rangle_z^{1/2}$, the power law describing the relationship between M_w and $\langle S^2\rangle_z^{1/2}$ ($\langle S^2\rangle_z^{1/2} \propto M_w^{\alpha}$) can be created. Usually, the chain conformation of the polymer in solution can be estimated by the value of exponent (α). Usually, the α value is 0.3 for globular shape, 0.5−0.6 for flexible chain conformation in good solvent, and 0.6−1 for a semi-flexible or stiff chain (*30*). The log−log plots of $\langle S^2\rangle_z^{1/2} \propto M_w^{\alpha}$ for GL-IV-I in Me_2SO and its derivatives in 0.9% NaCl are shown in **Figure 4**. The α value for GL-IV-I was 0.47, indicating that the glucans existed as a flexible

Table 3. Experiment Results from LLS, SEC−LLS, and Viscosity for GL-IV-I and Its Derivatives

		LLS			SEC−LLS			
sample	solvent	M_w ($\times 10^{-4}$) (g mol^{-1})	A_2 ($\times 10^4$) (mol mL g^{-2})	$\langle S^2\rangle_z^{1/2}$ (nm)	M_w ($\times 10^{-4}$) (g mol^{-1})	M_w/M_n	α	[η] (cm^3 g^{-1})
GL-IV-I	Me_2SO	12.4	3.67	53.5	13.3	1.37	0.47	27.8
S-GL	0.9% NaCl	12.5	2.14	56.6	10.1	1.86	0.61	29.3
CM-GL	0.9% NaCl	5.2	3.56	35.7	6.3	1.62	0.56	39.7

Table 4. Results of *in Vivo* Antitumor Activities and the Enhancement Ratio of the Body Weight of S-GL and CM-GL Compared to 5-Fu[a]

sample	dose (mg/kg × days)	inhibition ratio (%)	enhancement ratio of body weight (%)	complete repression
S-GL	40 × 8	55.6 ± 2.1	48.5 ± 1.5	0/8
CM-GL	40 × 8	51.3 ± 1.3	45.7 ± 2.7	0/8
5-Fu	40 × 8	61.9 ± 3.8	28.2 ± 1.7[b]	0/8
0.9% NaCl	40 × 8		46.4 ± 2.7	0/8

[a] Results are expressed as mean ± SD (n = 8). [b] $p < 0.01$ (Dunnett's test).

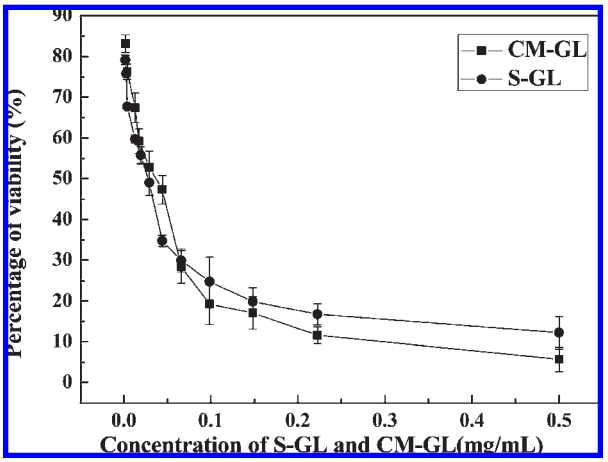

Figure 5. Percentage of viability of S-180 cells treated with sulfated (S-GL) and carboxymethylated (CM-GL) derivatives of GL-IV-I at different concentrations. Data are shown as mean ± standard deviation (SD) (n = 3).

chain conformation in Me_2SO at 25 °C. The α values for S-GL and CM-GL were 0.61 and 0.56, respectively. This suggested that the chain stiffness of the two derivatives was slightly higher than that of the native glucan. Namely, the derivatives existed as relatively expanded flexible chains in 0.9% NaCl aqueous solution at 25 °C, as a result of the steric hindrance of the substituted groups in S-GL and CM-GL. The introduction of the charged groups, such as sulfated and carboxymethylated groups, improved the water solubility and increased the chain stiffness.

Antiproliferative Effect of S-GL and CM-GL on S-180. The antiproliferative effect of S-GL and CM-GL on the S-180 tumor cell line was investigated. Cells were treated at different concentrations of these two derivatives (0−500 μg/mL) for 24 h. **Figure 5** shows the percentage of viability of S-180 cells in the presence of S-GL and CM-GL with different concentrations. Cells incubated with 0.2% Me_2SO were used as a control. The median inhibitory concentration (IC_{50}) values of S-GL and CM-GL tested against S-180 cancer cells were 26 and 38 μg/mL after 24 h of treatment. Therefore, S-GL and CM-GL could inhibit the *in vitro* proliferation of S-180 tumor cells in a dose-dependent manner.

***In Vivo* Antitumor Activities.** To investigate the antitumor activities of S-GL and CM-GL, the sample solutions were injected intraperitoneally (40 mg/kg) once daily for 8 days after S-180 tumor cell inoculation for 24 h. The inhibitions of tumor growth *in vivo* and enhancement ratio of body weight are summarized in **Table 4**. The native GL-IV-I showed no antitumor activity because of the poor water solubility. However, the inhibition ratios of S-GL and CM-GL were 55.6 ± 2.1 and 51.3 ± 1.3%, respectively. The growth of the S-180 solid tumors was markedly inhibited by S-GL and CM-GL. It is worth noting that the two derivatives exhibited relatively high inhibition on the tumor growth, only slightly lower than that of 5-Fu. **Figure 6** shows pictures of the tumors of the control group treated with 0.9% NaCl aqueous solution and the experimental groups treated with S-GL and CM-GL. Although the 5-Fu group exhibited more effective results, its body weight enhancement ratio was 28.2 ± 1.7%, which was much lower than that of S-GL and CM-GL groups (48.5 ± 1.5 and 45.7 ± 2.7%, respectively). Besides, the enhancement ratio of the body weight of mice treated with S-GL and CM-GL groups was almost equal to the control group. Therefore, our findings indicated that S-GL and CM-GL are potential antitumor agents, having high bioactivities and low toxicity. S-GL had a lower IC_{50} value than that of CM-GL, implying that the introduction of sulfated groups is more conducive to the enhancement of the antitumor activity of the polysaccharides.

Cell-Cycle Arrest and Apoptosis Induction by Polysaccharides. Apoptosis is a physiological and crucial process that is regarded as the preferred way to eliminate cancer cells (*31*, *32*). **Figure 7** shows the effect of (**a**) CM-GL and (**b**) S-GL on the cell-cycle phases (G_0/G_1, S, and G_2/M) of S-180 cells. S-GL and CM-GL induced accumulation of S-180 cells in the sub-G_1 peak, indicating apoptotic phenomenon, as well as led to the G_2/M phase arrest. In the cell-cycle analysis, a significant increase of the cell population in the G_2/M phase was observed from 16.1 ± 1.4% of the control group to 33.5 ± 2.4% for S-GL and 29.7 ± 1.5% for CM-GL, with the concentration of 0.02 mg/mL. These results suggested that the S-GL and CM-GL derivatives could inhibit the growth of S-180 cells through cell-cycle arrest in the G_2/M phase and induced the apoptosis. **Figure 8** shows representative dot plots of fluorescence intensities of S-180 cells labeled with Annexin V/PI. The percentage of surviving (Annexin V and PI negative, AnVK/PIK) and apoptotic (Annexin V positive and PI negative, AnVC/PIK) cells was indicated in the quadrants. The percentage of apoptosis in control S-180 cells (2.57 ± 0.39%) was significantly ($p < 0.05$) lower than that of S-GL (17.9 ± 1.98%) and CM-GL (14.1 ± 2.67%). Treatment with S-GL and CM-GL resulted in a significant increase in the percent of apoptosis of S-180 cells. The percentage of surviving cells in the three groups was inversely related to the percentages of apoptotic cells. In view of the results, S-GL and CM-GL exhibited a significant increase of apoptosis and decrease in the survival of S-180 cells.

The proto-oncogene Bcl-2 protects cells against apoptosis, whereas Bax promotes cells against apoptosis (*33*).

Figure 6. Mice injected with sulfated (S-GL) and carboxymethylated (CM-GL) derivatives of GL-IV-I or 5-Fu intraperitoneally had significantly smaller tumor volumes compared to control mice on day 8. Average tumor weights of mice treated with S-GL or CM-GL were significantly reduced compared to that in the control group.

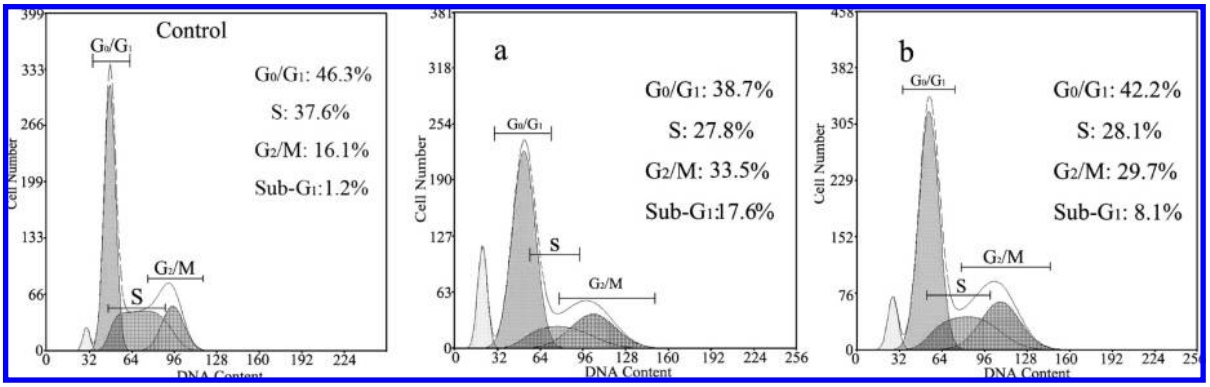

Figure 7. Representative cytograms show the effect of (a) sulfated (S-GL) and (b) carboxymethylaed (CM-GL) derivatives of GL-IV-I on the cell-cycle phases (G_0/G_1, S, and G_2/M) and apoptosis (sub-G_1) of S-180 cells. The cells were incubated for 24 h without (control) and with S-GL and CM-GL at a final concentration of 0.02 mg/mL.

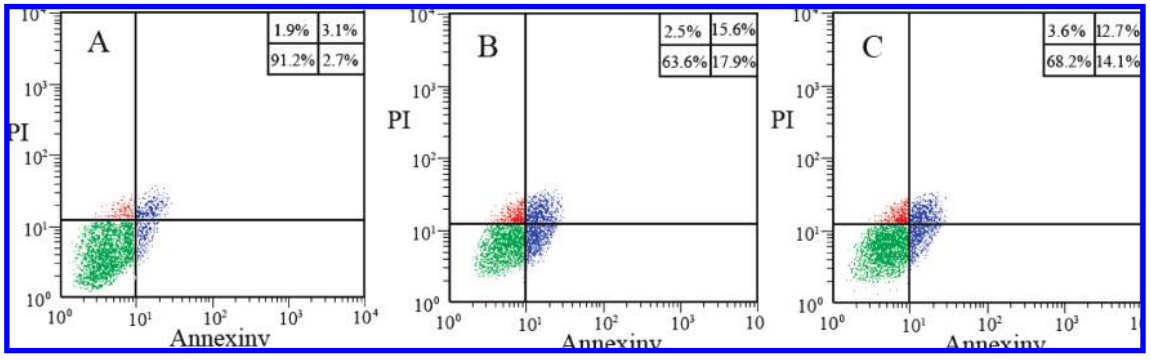

Figure 8. Fluorescence-activated sorting analysis of Annexin V and PI for induced apoptosis in S-180 cells treated with sulfated (S-GL) and carboxymethylaed (CM-GL) derivatives of GL-IV-I. The percentage of apoptosis was determined by flow cytometry. (A) Control S-180 cells. (B and C) Cells after 24 h of treatment with S-GL and CM-GL (0.02 mg/mL), respectively. The data shown are representative of three independent experiments.

We investigated alterations in the expression of apoptosis-related proteins Bcl-2 and Bax in S-180 tumor treated by intraperitoneal injection of the S-GL and CM-GL aqueous solution into BALB/c female mice. **Figures 9** and **10** show the apoptosis-related proteins Bax and Bcl-2 immunostain in S-180 tumor of the untreated control mice, 5-Fu group, and S-GL and CM-GL treated mice. The results revealed a significant difference in the expression of the proteins in the control and S-GL and CM-GL groups. In the control group, Bax was not detected, whereas Bcl-2 immunostain was strong in the S-180 tumor. However, the mice treated with S-GL and CM-GL exhibited a significantly decreased expression of Bcl-2 and increased expression of Bax. The uniquely high Bax expression with low Bcl-2 immunostain indicated that the polysaccharide derivatives induced apoptosis of S-180 tumor cells probably by upregulating the expression of Bax to counteract the effect of Bcl-2. The results from the quantitative analysis of the Bax and Bcl-2 immunostain for the S-180 tumor in the control and S-GL and CM-GL groups are summarized in **Table 5**. The expression levels of the two apoptotic proteins led to a significantly lower Bcl-2/Bax ratio, suggesting a favorable therapeutic response to S-GL and CM-GL and an increase of the survival rate in mice transplanted with S-180 tumors. Furthermore, a high expression level of Bax accompanied by a low Bcl-2 immunoreactivity could sustain a low Bcl-2/Bax ratio in favor of apoptosis,

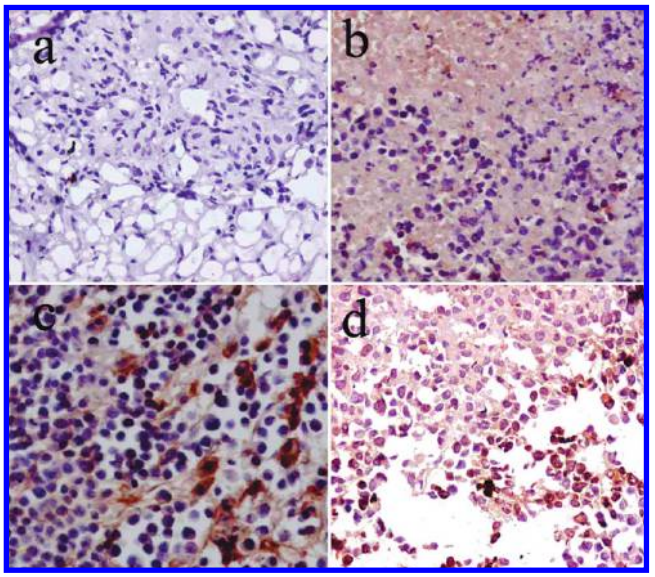

Figure 9. Bax immunostain in S-180 tumor of the (a) untreated control mice, (b) 20 mg/kg S-GL treated mice, (c) 40 mg/kg CM-GL treated mice, and (d) 20 mg/kg 5-F treated mice. S-GL and CM-GL are sulfated and carboxymethylaed derivatives of GL-IV-I, respectively.

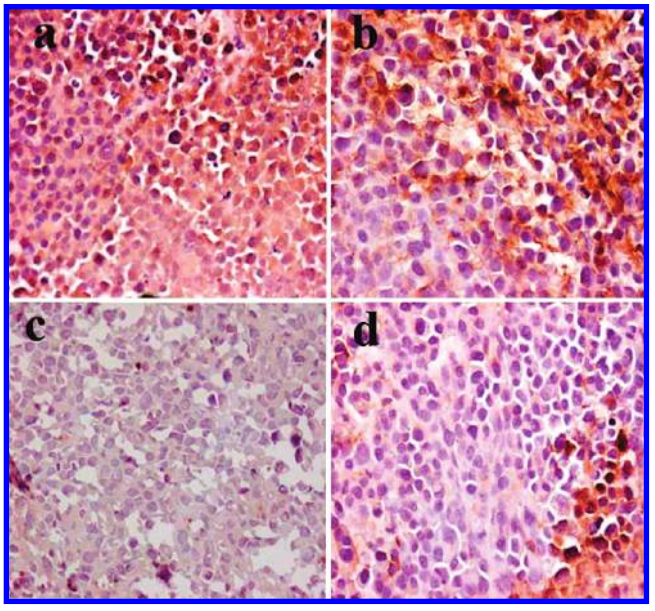

Figure 10. Bcl-2 immunostain in S-180 tumor of the (a) untreated control mice, (b) 20 mg/kg S-GL treated mice, (c) 40 mg/kg CM-GL treated mice, and (d) dose 20 mg/kg 5-F treated mice. S-GL and CM-GL are sulfated and carboxymethylaed derivatives of GL-IV-I, respectively.

or alternatively, it could effectively antagonize the anti-apoptotic levels of the Bcl-2. The immuno-histochemical results indicated that both S-GL and CM-GL could induce apoptosis in xenograft S-180 tumor cells by upregulating Bax and downregulating Bcl-2, while S-GL showed a better therapeutic effect than CM-GL.

On the basis of the results mentioned above, the water-soluble derivatives of polysaccharides having charged groups and relatively expanded chain conformation exhibited high antitumor activity. Therefore, the introduction of the sulfated and carboxymethylated groups could improve the water solubility and increase the chain stiffness, leading to the enhancement of the antitumor activities. The relatively extended chain conformation of carboxymethylated β-glucan from sclerotium of *P. tuber-regium* and extracellular polysaccharides from *Ganoderma tsugae mycelium* correlated with their relatively higher antitumor activity. This could be explained by the fact that charged groups and relatively expanded flexible chains of polysaccharides have more opportunities to bind with receptors on the cell than the compact conformation.

Table 5. Quantitative Analysis of the Bax and Bcl-2 Immunostaining for S-180 Tumor Cells in the Control and AAG-Treated Groups[a]

samples	Bax (% immunoreactivity)	Bcl-2 (% immunoreactivity)
control group	3.8 ± 1.3	58.5 ± 4.2
5-Fu dose 40 mg/kg	30.3 ± 3.5^b	21.8 ± 2.7^b
S-GL dose 40 mg/kg	46.5 ± 2.9^b	39.6 ± 3.1^c
CM-GL dose 40 mg/kg	42.6 ± 3.6^b	30.7 ± 2.4^b

[a] Results are expressed as mean $\pm$ SD (n = 8). [b] $p < 0.01$ (Dunnett's test). [c] $p < 0.05$ (Dunnett's test).

ACKNOWLEDGMENT

We thank Professor Zeng of Tongji Medical College of Huazhong University of Science and Technology for his kind help.

LITERATURE CITED

(1) Zhang, C.; Huang, K. Mechanism of apoptosis induced by a polysaccharide, from the loach *Misgurnus anguillicaudatus* (MAP) in human hepatocellular carcinoma cells. *Toxicol. Appl. Pharmacol.* **2006**, *210*, 236–245.

(2) Wasser, S. P. Medicinal mushrooms as a source of anti-tumor and immuno-modulating polysaccharides. *Appl. Microbiol. Biol.* **2002**, *60*, 258–274.

(3) Yang, X. B.; Zhao, Y.; Yang, Y.; Ruan, Y. Isolation and characterization of immunostimulatory polysaccharide from an herb tea, *Gynostemma pentaphyllum* Makino. *J. Agric. Food Chem.* **2008**, *56*, 6905–6909.

(4) Zhu, J. F.; Wu, M. Characterization and free radical scavenging activity of rapeseed meal polysaccharides WPS-1 and APS-2. *J. Agric. Food Chem.* **2009**, *57*, 812–819.

(5) Tommonaro, G.; Segura Rodríguez, C. S.; Santillana, M.; Immirzi, B.; De Prisco, R.; Nicolaus, B.; Poli, A. Chemical composition and biotechnological properties of a polysaccharide from the peels and antioxidative content from the pulp of *Passiflora liguralis* fruits. *J. Agric. Food Chem.* **2007**, *55*, 7427–7433.

(6) Cheng, Y. L.; Lee, S. C.; Lin, S. Z.; Chang, W. L.; Chen, Y. L.; Tsai, N. M.; Liu, Y. C.; Tzao, C.; Yu, D. S.; Harn, H. J. Anti-proliferative activity of *Bupleurum scrozonerifolium* in A549 human lung cancer cells *in vitro* and *in vivo*. *Cancer Lett.* **2005**, *222*, 183–193.

(7) Li, G.; Kim, D.-H.; Kim, T.-D.; Park, B.-J.; Park, H.-D.; Park, J.-I.; Na, M.-K.; Kim, H.-C.; Hong, N.-D.; Lim, K.; Hwang, B.-D.; Yoon, W.-H. Protein-bound polysaccharide from *Phellinus linteus* induces G_2/M phase arrest and apoptosis in SW480 human colon cancer cells. *Cancer Lett.* **2004**, *216*, 175–181.

(8) Cao, L.; Lin, Z. Regulation on maturation and function of dendritic cells by *Ganoderma lucidum* polysaccharides. *Immunol. Lett.* **2002**, *83*, 163–169.

(9) Nie, X.; Shi, B.; Ding, Y.; Tao, W. Preparation of a chemically sulfated polysaccharide derived from *Grifola frondosa* and its potential biological activities. *Int. J. Biol. Macromol.* **2006**, *39*, 228–233.

(10) Huang, Q.; Zhang, L. Solution properties of (1 → 3)-α-D-glucan and its sulfated derivertives from *Poris cocos* mycelis via fermentation tank. *Biopolymers* **2005**, *79*, 28–38.

(11) Zhang, M.; Zhang, L.; Cheung, P. C. K. Molecular mass and chain conformation of carboxymethylated derivatives of β-D-glucan from sclerotia of *Pleurotus tuber-regium*. *Biopolymers* **2003**, *68*, 150–159.

(12) Zhang, M.; Zhang, P. C. K.; Zhang, L.; Chiu, C. M.; Ooi, V. E. C. Carboxymethylated β-glucan from mushroom sclerotium of *Pleurotus tuber-regium* as novel water-soluble anti-tumor agent. *Carbohydr. Polym.* **2004**, *57*, 319–325.

(13) Wang, J.; Zhang, L. Structure and chain conformation of five water-soluble derivatives of β-D-glucan isolated from *Ganoderma lucidum*. *Carbohydr. Res.* **2009**, *344*, 105–112.

(14) Yoshida, T.; Yasuda, Y.; Mimura, T.; Kaneko, Y.; Nakashima, H.; Yamamoto, N.; Uryu, T. Synthesis of curdlan sulfates having inhibitory effects in vitro against AIDS viruses HIV-1 and HIV-2. *Carbohydr. Res.* **1995**, *276*, 425–436.
(15) Bao, X.; Duan, J.; Fang, X.; Fang, J. Chemical modifications of the (1 → 3)-α-D-glucan from spores of *Ganoderma lucidum* and investigation of their physicochemical properties and immunological activity. *Carbohydr. Res.* **2001**, *336*, 127–140.
(16) Qiu, H.; Tang, W.; Tong, X.; Ding, K.; Zuo, J. Structure elucidation and sulfated derivatives preparation of two α-D-glucans from *Gastrodia elata* Bl. and their anti-dengue virus bioactivities. *Carbohydr. Res.* **2007**, *342*, 2230–2236.
(17) Lohmann, C. M.; League, A. A.; Clark, W. S.; Lawson, D.; DeRose, P. B.; Cohen, C. Bcl-2:Bax and Bcl-2:Bcl-x ratios by image cytometric quantitation of immunohistochemical expression in ovarian carcinoma: Correlation with prognosis. *Cytometry* **2000**, *42*, 61–66.
(18) Saxena, A.; McMeekin, J. D.; Thomson, D. J. Expression of Bcl-x, Bcl-2, Bax, and Bak in endarterectomy and atherectomy specimens. *J. Pathol.* **2002**, *196*, 335–342.
(19) Xie, X.; Clausen, O. P. F.; Angelis, P. D.; Boysen, M. The prognostic value of spontaneous apoptosis, Bax, Bcl-2, and p53 in oral squamous cell carcinoma of the tongue. *Cancer Lett.* **1999**, *86*, 913–920.
(20) Kiho, T.; Sakushima, M.; Wang, S.; Nagai, K.; Ukai, S. Polysaccharides in fungi. XXVI. Two branched (1,3)-β-D-glucans from hot water extract of yuer. *Chem. Pharm. Bull.* **1991**, *39*, 798–880.
(21) Zhang, M.; Zhang, L.; Chen, J.; Zeng, F. Solution properties of antitumor sulfated derivatives of (1 → 3)-α-D-glucan from *Ganoderma lucidum*. *Biosci., Biotechnol., Biochem.* **2000**, *64*, 2172–2178.
(22) Wang, Y.; Zhang, L.; Li, Y.; Hou, X.; Zeng, F. Correlation of structure to antitumor activities of five derivatives of a β-glucan from *Poria cocos* sclerotium. *Carbohydr. Res.* **2004**, *339*, 2567–2574.
(23) Jin, Y.; Zhang, H.; Yin, Y.; Nishinari, K. Comparison of curdlan and its carboxymethylated derivative by means of rheology, DSC, and AFM. *Carbohydr. Res.* **2006**, *341*, 90–99.
(24) Zhang, L.; Zhang, M.; Chen, J. Solution properties of antitumor carboxymethylated derivertives of (1 → 3)-α-D-glucan from *Ganoderma lucidum*. *Chin. J. Polym. Sci.* **2001**, *19*, 283–289.
(25) Wang, Y.; Zhang, L.; Ruan, D. Preparation and structure of five derivertives of (1 → 3)-β-D-glucan isolated from *Poria cocos* sclerotium. *Chin. J. Polym. Sci.* **2004**, *22*, 137–145.
(26) Kato, T.; Okamoto, T.; Tokuya, T.; Takahashi, A. Solution properties and chain flexibility of pullulan in aqueous solutions. *Biopolymers* **1982**, *21*, 1623–1633.
(27) Zhou, J.; Zhang, L.; Deng, H.; Wu, X. Synthesis and characterization of cellulose derivatives prepared in NaOH/urea aqueous solutions. *J. Polym. Sci., Part A: Polym. Chem.* **2004**, *42*, 5911–5920.
(28) Gorin, P. A. J. Carbon-13 nuclear magnetic resonance spectroscopy of polysaccharides. *Adv. Carbohydr. Chem. Biochem.* **1981**, *38*, 13–104.
(29) Picton, L.; Bataille, G.; Muller, G. Analysis of a complex polysaccharide (gum arabic) by multi-angle laser light scattering coupled on-line to size exclusion chromatography and flow field flow fractionation. *Carbohyd. Polym.* **2000**, *42*, 23–31.
(30) Chen, X.; Xu, X.; Zhang, L.; Zeng, F. Chain conformation and antitumor activities of phosphorylated (1 → 3)-β-D-glucan from *Poria cocos*. *Carbohydr. Polym.* **2009**, *78*, 581–587.
(31) Sogawa, K.; Yamada, T.; Sumida, T.; Hamakawa, H.; Kuwabara, H.; Matsuda, M. Induction of apoptosis and inhibition of DNA topoisomerase-I in K-562 cells by a marine microalgal polysaccharide. *Life Sci.* **2000**, *66*, 227–231.
(32) Zhang, C.; Huang, K. Apoptosis induction on HL-60 cells of a novel polysaccharide from the mucus of the loach, *Misgurnus anguillicaudatus*. *J. Ethnopharmacol.* **2005**, *99*, 385–390.
(33) Tsujimoto, Y.; Crose, C. M. Analysis of the structure, transcripts, and protein products of Bcl-2, the gene involved in human follicular lymphoma. *Proc. Natl. Acad. Sci. U.S.A.* **1986**, *83*, 5214–5218.

Received for review July 27, 2009. Revised manuscript received October 7, 2009. Accepted October 7, 2009. We gratefully acknowledge the major grants of the National Natural Science Foundation of China (30530850), the National Natural Science Foundation (20874079), and the High-Technology Research and Development Program of China (2006AA02Z102).